American Journal of Engineering Research (AJER)
e-ISSN : 2320-0847 p-ISSN : 2320-0936
Volume-02, Issue-07, pp-213-226
www.ajer.org

Research Paper Open Access

Image Classifying Registration and Dynamic Region Merging

Himadri Nath Moulick, Moumita Ghosh
CSE, Aryabhatta Institute of Engg & Management, Durgapur, PIN-713148, India
CSE, University Institute Of Technology,(The University of Burdwan) Pin -712104,India

Abstract: - In this paper, we address a complex image registration issue arising when the dependencies between intensities of images to be registered are not spatially homogeneous. Such a situation is frequently encountered in medical imaging when a pathology present in one of the images modifies locally intensity dependencies observed on normal tissues. Usual image registration models, which are based on a single global intensity similarity criterion, fail to register such images, as they are blind to local deviations of intensity dependencies. Such a limitation is also encountered in contrast enhanced images where there exist multiple pixel classes having different properties of contrast agent absorption. In this paper, we propose a new model in which the similarity criterion is adapted locally to images by classification of image intensity dependencies. Defined in a Bayesian framework, the similarity criterion is a mixture of probability distributions describing dependencies on two classes. The model also includes a class map which locates pixels of the two classes and weights the two mixture components. The registration problem is formulated both as an energy minimization problem and as a Maximum A Posteriori (MAP) estimation problem. It is solved using a gradient descent algorithm. In the problem formulation and resolution, the image deformation and the class map are estimated at the same time, leading to an original combination of registration and classification that we call image classifying registration. Whenever sufficient information about class location is available in applications, the registration can also be performed on its own by fixing a given class map. Finally, we illustrate the interest of our model on two real applications from medical imaging: template-based segmentation of contrast-enhanced images and lesion detection in mammograms. We also conduct an evaluation of our model on simulated medical data and show its ability to take into account spatial variations of intensity dependencies while keeping a good registration accuracy. And the addresses the automatic image segmentation problem in a region merging style. With an initially over-segmented image, in which the many regions (or super-pixels) with homogeneous color are detected, image segmentation is performed by iteratively merging the regions according to a statistical test. There are two essential issues in a region merging algorithm: order of merging and the stopping criterion. In the proposed algorithm, these two issues are solved by a novel predicate, which is defined by the sequential probability ratio test (SPRT) and the minimal cost criterion. Starting from an over-segmented image, neighboring regions are progressively merged if there is an evidence for merging according to this predicate. We show that the merging order follows the principle of dynamic programming. This formulates image segmentation as an inference problem, where the final segmentation is established based on the observed image. We also prove that the produced segmentation satisfies certain global properties. In addition, a faster algorithm is developed to accelerate the region merging process, which maintains a nearest neighbor graph (NNG) in each iteration. Experiments on real natural images are conducted to demonstrate the performance of the proposed dynamic region merging algorithm.

Keywords: - *Image segmentation, Region merging, Wald's SPRT, Dynamic programming, Image registration, mixture models, lesion detection.*

I. INTRODUCTION

Image registration is a central issue of image processing, which is particularly encountered in medical applications [1]–[5]. Medical image registration is critical for the fusion of complementary information about patient anatomy and physiology, for the longitudinal study of a human organ over time and the monitoring of disease development or treatment effect, for the statistical analysis of a population variation in comparison to a

so-called digital atlas, for image-guided therapy, etc. Image registration consists in mapping domains of several images onto a common space and results in some corrections of geometric differences between the images. Most of classical registration techniques rely upon the assumption that there exists a relationship between intensities of images to be registered and that this relationship remains the same all over the image domains [6]–[11]. This assumption is typically made when applying registration techniques based on intensity criteria such as the sum of squared differences, the correlation ratio, the correlation coefficient or the mutual information [10]. But such an assumption is not always satisfied. As an example, let us mention the medical imaging case when a contrast agent is used to enhance some pathological tissues (lesions) [12], [13]. After enhancement, intensities of normal tissues and lesions are likely to differ, even though they can be the same before enhancement. So, a same intensity before enhancement may correspond to several intensities after enhancement. Hence, with contrast-enhanced imaging modalities, the relationship between image intensities is neither unique, nor spatially invariant. It mainly depends on the type of observed tissues. In such cases, ignoring the spatial context may lead to locally establishing an inaccurate or even inconsistent correspondence between homologous geometric structures. This issue was documented in [13], [14],

where it is shown that such non-rigid registration would wrongly change the size of non-deformed contrast-enhanced structures. In the literature, there have been several works dealing with image registration in the presence of multiple pixel classes. These works can mainly be divided into two categories: those based on robust estimation and mixture models, and those combining registration and classification (or segmentation). Robust estimation is a statistical approach which has been widely applied to image processing [15]. This approach involves the definition of outliers, which are characterized as elements deviating from a normal model, detected and possibly rejected [16]–[19]. Applied to optical flow estimation and image registration [20]–[25], robust estimation helps to reduce the influence of large insignificant image differences on the optical flow or the deformation estimation. However, these approaches offer poor characterizations of outliers, which are usually described as pixels generating large image differences. They cannot deal with complex situations arising from medical imaging applications. More general robust estimation approaches are based on mixture models [18] and characterize outliers by some specific probability distributions [26]–[34]. In optical flow computation, a mixture model was used to distinguish between several layers of movements and an outlier class [31]. In image registration, some authors used a mixture model in which image differences generated by outliers are represented by a mixture component [29], [30]. Similar approaches could be used in medical image registration considering medical lesions as outliers [26]–[28]. However, the main and important difference with the model we introduce in this paper is that the mixture models proposed above do not use any spatial and geometric information about the pixel classes but only pixel-independent mixing proportions. In other approaches, spatial informations derived from segmentation were used to adapt regionally the similarity criterion describing intensity relationships [35]–[38]. Such segmentation-based approaches require a preliminary segmentation of the images which, obviously, cannot always be obtained. For instance, in dynamic contrast-enhanced sequences, the image segmentation has to be estimated from the registered images [39]. Image segmentation has also been combined with atlas-based registration in Bayesian frameworks [40], [41], where mixture models were used to represent pixel intensities of different anatomical structures. In other works, Markov random fields were employed to describe a label map of pixel classes. The registration and the segmentation were then computed by the Maximum A Posteriori (MAP) estimation [42]–[44]. In such approaches, one can incorporate prior information about the lesion shape and localization. However, the proposed methods used simple characterizations of intensity variations. In this paper, we deal with the issue of registering images whose intensity relationship is spatially dependent. We propose a new technique where the registration is simultaneously combined to a pixel classification. This classification provides some spatial information about intensity relationships. We use

Mixture models to take into account complex intensity changes and Markov random fields to label pixels. The paper is organized as follows. Section 2 describes the theoretical foundation of the proposed new method. Then, the numerical aspects are discussed in Section 3. In Section 4, experiments are conducted both on simulated and on real data to evaluate the method performance. Finally, some conclusions and possible extensions of the proposed approach are discussed in the last section. Image segmentation is a fundamental yet still challenging problem in computer vision and image processing. In particular, it is an essential process for many applications such as object recognition, target tracking, content-based image retrieval and medical image processing, etc. Generally speaking, the goal of image segmentation is to partition an image into a certain number of pieces which have coherent features (color, texture, etc.) and in the meanwhile to group the meaningful pieces together for the convenience of perceiving [61]. In many practical applications, as a large number of images are needed to be handled, human interactions involved in the segmentation process should be as less as possible. This makes automatic image segmentation techniques more appealing. Moreover, the success of many high-level segmentation techniques (e.g. class-based object segmentation [82, 83]) also demands sophisticated automatic segmentation techniques. Dating back over decades, there is a large amount of literature

on automatic image segmentation. For example, the edge detection algorithms [74-79] are based on the abrupt changes in image intensity or color, thus salient edges can be detected. However, due to the resulting edges are often discontinuous or over-detected, they can only provide candidates for the object boundaries. Another classical category of segmentation algorithms is based on the similarities among the pixels within a region, namely region-based algorithms. In order to cluster the collection of pixels of an image into meaningful groups of regions or objects, the region homogeneity is used as an important segmentation criterion. Many cut criteria in graph theory have been studied for this purpose. The most widely used cut criteria include normalized cut [88], ratio cut [9], minimum cut [10] and so on. The aim of these algorithms is to produce a desirable segmentation by achieving global optimization of some cost functions. However, these cost functions only provide a

Characterization of each cut rather than the whole regions. Another problem is that the optimization processes are often computationally inefficient for many practical applications. In recent years, the success of combinatorial graph cut methods [71-72] has been attracting significant research attention. These methods utilize the user input information along with the cut criteria in optimization and nearly global optima can be achieved in linear computational time. As a matter of fact, for most cut-based energy functionals a single optimal partition of an image is not easy to obtain. It makes a possibility of finding different level-based explanations of an image. From this aspect, there are methods [81-82] tackling the image segmentation as a hierarchical bottom-up problem. In region-based methods, a lot of literature has investigated the use of primitive regions as a preprocessing step for image segmentation [83-85]. The advantages are twofold. First, regions carry on more information in describing the nature of objects. Second, the number of primitive regions is much fewer than that of pixels in an image and thus largely speeds up the region merging process. Starting from a set of primitive regions, the segmentation is conducted by progressively merging the similar neighboring regions according to a certain predicate, such that a certain homogeneity criterion is satisfied. In previous works, there are region merging algorithms based on statistical properties [66, 72-73, 70-71], graph properties [87-89, 74-75] and spatio-temporal similarity [80]. Although the segmentation is obtained by making local decisions, some techniques [66-71] have shown satisfying results with efficient implementation. Most region merging algorithms do not have some desirable global properties, even though some recent works in region merging address the optimization of some global energy terms, such as the number of labels [90] and the area of regions [91]. As a good representation of morphological segmentation, watershed transform [92] can also be classified as region-based segmentation methods. The intuitive idea comes from geography, where watersheds are the dividing lines of different catchment basins. The major drawback of watershed transform is the over-segmentation of the image. To overcome this problem, one solution is "flooding" from the selected markers [76-78] such that only the most important regional minima are saved for the segmentation. The other [79] is based on a hierarchical process, where the catchment basins of the watershed image are merged until they belong to almost homogeneous regions. In this paper, we implement the segmentation algorithm in a region merging style for its merit of efficiency, where similar neighboring regions are iteratively merged according to a novel merging predicate. As stated above, homogeneity criteria (cues) are essential to the region merging process. Although a good enough cue is needed in order to obtain a valuable segmentation, our work does not focus on finding a more complex region model. Instead, we model the cues by a function of random variables. In this way, the properties of cues are not mainly concerned, but the reliability of the cues. In many traditional segmentation algorithms (e.g. [63-69]), the reliability is predetermined and thus researchers often try to use more reliable cues for implementation. In contrast, some statistical segmentation methods are able to calculate the reliability of cues, for example, using the parametric probability models [80-81]. But they cannot be used in a general scenario. Another statistical method [76] directly uses the statistical property of image data (e.g., colors) to identify the region border. Particularly, a homogeneity criterion is proposed based on the expectation of pixel colors inside a region, which naturally leads to a merging predicate. In the recent work of region merging [72], a likelihood ratio test is applied as the measure of region similarity. The probability of adjacent regions and that of their merging are both computed. To minimize both probabilities of error, the optimal merging will take place along with the largest decreasing of the likelihood ratio.

II. THE BAYESIAN FRAMEWORK

Let m and n be two integers, and Ω_d = {0, ...,m − 1} × {0, ..., n − 1} be a discrete grid of size N = m n. Observed images are real-valued functions defined on d. They can be interpolated on the continuous domain Ω = [0,m − 1] × [0, n − 1] naturally associated to the grid d. For convenience, elements of Ω_d are ordered and will be denoted xi for i = 1, · · · ,N. The registration of two images I and J consists in finding a mapping _ : ϕ : $\Omega \rightarrow \Omega$ for which the

deformed image Iφ := I ϕ of the so-called source image I is as similar as possible to the so-called target image J.

In a Bayesian framework, the mapping _ is usually obtained as a MAP estimate (see [45] and references therein). Specific to this framework, images and deformations are assumed to be some realizations of random fields indexed on Ω_d and Ω, respectively. For each point xi of Ω_d, I(xi) and J(xi) are realizations of two real-valued random variables and, for each point x of , Ω, (x) is a realization of a random vector with values in . The relationships between the intensities of the registered images are then statistically described by a probability distribution of J given I, ϕ and a set of parameters θ (this conditional distribution is denoted by π (J | I, $I, \phi; \theta$)). Usually, the variables J(xi) are assumed to be independent conditionally to the variables Iφ(xi). Hence, ($\pi(J \mid I, \phi; \theta)$) can be written as

$$\pi(J \mid I, \phi; \theta) = \prod_{i=1}^{N} \pi(J(x_i) \mid I^{\phi}(x_i); \theta). \quad (1)$$

Because of noise, and also because it is a very generic choice, it is possible to assume that the intensity differences between J(x) and Iφ(x) follow a Gaussian distribution with mean μ and variance σ^2 at each pixel x ∈ $\Omega_{d:}$, leading to the distribution

$$\pi(J(x) \mid I^{\phi}(x); \theta) = \frac{1}{\sqrt{2\pi}\sigma} \exp\left(-\frac{1}{2\sigma^2}(J(x) - I^{\phi}(x) - \mu)^2\right), \quad (2)$$

with $\theta = (\mu, \sigma)$ In this definition, it is worth noticing that the mean μ and the variance σ^2 do not depend on any position x. Consequently, the intensity relationship between images is spatially homogeneous. Let us further mention that, similarly to this particular Gaussian distribution, distributions associated to other usual criteria (e.g. correlation ratio, correlation coefficient, or mutual information) are also homogeneous. Besides, a prior probability distribution is set on the mappings _ in order to favour smooth deformations as solutions of the registration problem. Let $\phi = \mathrm{id} + u$ be written as the sum of the identity map id and a displacement field u, seen as an element of a Hilbert space H equipped with an inner product a(·, ·). Let then ˜H be a finite-dimensional approximation subspace of H which is spanned by a basis $\mathcal{B} = (\psi_i)_{i=1}^{n_e}$, with ne ∈ N∗. In ˜H, a displacement u is uniquely determined by a vector of coefficients $\mathbf{b} = (\beta_i)_{i=1}^{n_e}$ such that $u = \sum_{i=1}^{n_e} \beta_i \cdot \psi_i$. In the following, the deformations ϕ are assumed to be expanded into the subspace ˜H and identified with their decomposition coefficients b. We will also use the notation Ib instead of Iφ. Several choices are possible for the basis B: Fourier basis, sine and cosine transform basis functions, B-splines, piecewise affine or trilinear basis functions, wavelets (see [46] for a review), etc. We consider an inner product on ˜H, given by $a(u, u) = \mathbf{b}^T A \mathbf{b}$, where bT is the transpose of b, and A is a symmetric positive-definite matrix. On ˜H, we then define a centered multivariate normal distribution with covariance matrix A^{-1} given by

$$\pi(\mathbf{b}) = (2\pi)^{\frac{-n_e}{2}} \sqrt{\det(A^{-1})} e^{-\frac{1}{2}\mathbf{b}^T A \mathbf{b}}. \quad (3)$$

This prior distribution is used as a regularity term to enforce the smoothness of the deformations ϕ. A usual choice for a(·, ·) is the bilinear form

$$a(u, v) = \frac{1}{2} \int_{\Omega} \sum_{i,j=1}^{2} \frac{\lambda}{2} \left(\frac{\partial u_i(x)}{\partial y_i} \frac{\partial v_j(x)}{\partial y_j}\right) dy + \frac{1}{2} \int_{\Omega} \sum_{i,j=1}^{2} \frac{\mu}{4} \left(\frac{\partial u_i(x)}{\partial y_j} + \frac{\partial v_j(x)}{\partial y_i}\right)^2 dy, \quad (4)$$

defined for $\lambda > 0$ and $\mu > 0$, which is an inner product on the Sobolev space $H^1(\Omega;\mathbb{R}^2)$ and is related to the linearized strain energy of elastic materials [47]–[50]. We choose here the elastic regularization without aiming at a specific application, but knowing that this term enables to deal with many medical imaging applications. Other regularity terms could be better adapted to specific applications. They can be easily introduced in the proposed model. Other choices include the membrane energy [51], the bending energy [52], etc. The matrix A can also be estimated from the data using for instance EM algorithms with stochastic approximation [53], [54].

III. THE TWO-CLASS REGISTRATION MODEL

We now outline our new model. It is an extension of the model described in the previous section. The main feature is the introduction and the estimation of a pixel classification to take into account the spatial variations of the statistical relationships between the intensities of J and Iφ.

Intensity relationships In Equation (2), the probability distribution $\pi(J(x)|I^{\mathrm{b}}(x);\theta)$ describing the intensity relationship is spatially homogeneous. We now assume that the pixels of image J can be divided into two classes (labeled 0 and 1) where the intensity relationships are different and denoted respectively by $\pi_j(J(x)|I^{\mathrm{b}}(x);\theta_j)$, $j \in \{0,1\}$. Let also L(x) be the probability for a pixel x to belong to the class 1. Then, the intensity relationship at pixel x is described by the mixture distribution

$$\pi(J(x)|I^{\mathrm{b}}(x),L(x);\theta) = \pi_0(J(x)|I^{\mathrm{b}}(x);\theta_0)\,(1-L(x)) + \pi_1(J(x)|I^{\mathrm{b}}(x);\theta_1)\,L(x), \quad (5)$$

where $\theta = (\theta_0,\theta_1)$. Let us denote Li = L(xi) and L = (L1, · · · ,LN)T the vector of class probabilities on grid pixels. Assuming the conditional independence on grid points, we obtain the global conditional distribution

$$\pi(J|I^{\mathrm{b}},\mathbf{L};\theta) = \prod_{i=1}^{N}\left(\pi_0(J(x_i)|I^{\mathrm{b}}(x_i);\theta_0)\,(1-L_i) + \pi_1(J(x_i)|I^{\mathrm{b}}(x_i);\theta_1)\,L_i\right). \quad (6)$$

In an application of our model to lesion detection, the classification aims at distinguishing pixels on a lesion (class 1) from those outside any lesion (class 0). In contrast-enhanced images, the enhancement is more important on lesions than it is on normal tissues, leading to higher image differences on lesions. Assuming that the distributions are Gaussian on both classes, we can define distributions π_0 and π_1 as

in Equation (2) using two different sets of parameters: $\theta_0 = (\mu_0,\sigma_0)$ π_0 and $\theta_1 = (\mu_1,\sigma_1)$ with μ1 > μ0. Another possibility is, as in robust estimation, to consider elements of class 1 as outliers of class 0 and put no specific information on class 1 by defining π_1 as the uniform distribution

$$\pi_1(J(x)|I^{\mathrm{b}}(x);\theta_1) = \frac{1}{N_{\mathrm{gl}}}, \quad (7)$$

where Ngl is the number of possible gray-levels of J. Finally, we define a prior distribution on the class map L itself in order to introduce some constraints on the spatial homogeneity of the pixels of a same class. For that purpose, we equip the grid Ω_d with a neighborhood system (either a 4 or 8 neighborhood system) and assume that the class map L is a Markov random field on it [55]. We have considered two prior distributions on L. The first one is a Gaussian model, given by

$$\pi(\mathrm{L}) = \frac{1}{Z}\exp\left(-\alpha_1\sum_{i=1}^{N}L_i^2 - \alpha_2\sum_{\{i,j=1,\cdots,N;x_i\sim x_j\}}(L_i-L_j)^2\right), \quad (8)$$

where xi ∼ xj means that xi and xj are neighboring pixels, Z is a normalization constant, $\alpha_1 > 0$ and $\alpha_2 > 0$. The second model, which is a particular case of the Gaussian model when L is binary with range {0, 1}, is the Bernoulli model

$$\pi(\mathbf{L}) = \frac{1}{Z}\exp\left(-\alpha_1 \sum_{i=1}^{N} L_i + \alpha_2 \sum_{\{i,j=1,\cdots,N; x_i \sim x_j\}} L_i L_j\right) \quad (9)$$

where _ $\alpha_1 > 0$ and $\alpha_2 > 0$. If we let X = 2L − 1, this model is equivalent to the Ising model [56].In models (10) and (11), the parameter α_1 restricts the amount of pixels of the class 1, whereas the parameter α_2 enforces the spatial homogeneity of the classes.

Parameters The distributions defined above involve several parameters. In our application, we used the prior deformation distribution defined by Equation (4) and set manually the Lame constants λ and μ from experiments. We also set manually the mean μ0 and the variance σ_0 of the Gaussian distribution π_0 of the class 0, and the weights α_1 and α_2 of the Gaussian or Bernoulli model in Equations (10) and (11). The other parameters, which are the mean μ1 and the variance σ_1 of the Gaussian distribution π_1 on class 1, are estimated from the data. We assume that μ1 belongs to an interval [μmin, μmax] and σ_1 to another interval [_min, _max] and put, as a prior, uniform independent distributions of μ1 and σ_1 on these intervals. The parameter vector θ is decomposed as $\theta = (\theta_0, \theta_1)$, where $\theta_0 = (\mu_0, \sigma_0)$ is known and $\theta_1 = (\mu_1, \sigma_1)$ This parameter θ_1 is then estimated, together with the deformation and the classification by solving the following MAP estimation problem:

$$(\widetilde{\mathbf{b}}, \widetilde{\mathbf{L}}, \widetilde{\theta}_1) = \arg\max_{\mathbf{b},\mathbf{L},\theta_1} \pi(J|I, \mathbf{L}, \mathbf{b}; \theta_0, \theta_1)\, \pi(\mathbf{b})\, \pi(\mathbf{L})\, \pi(\theta_1). \quad (10)$$

As before, this is equivalent to the minimization of an energy of the form

$$\mathcal{E}(\mathbf{b}, \mathbf{L}, \theta_1) = S(I, J, \mathbf{b}, \mathbf{L}; \theta) + H(\mathbf{b}) + R(\mathbf{L}), \quad (11)$$

under the constraint that $\mu_1 \in [\mu_{min}, \mu_{max}]$ and $\sigma_1 \in [\sigma_{min}, \sigma_{max}]$.

IV. THE REGION MERGING PREDICATE

Automatic image segmentation can be phrased as an inference problem [60]. For example, we might observe the colors in an image, which are caused by some unknown principles. In the context of image segmentation, the observation of an image is given but the partition is unknown. In this respect, it is possible to formulate the inference problem as finding some representation of the pixels of an image, such as the label that each pixel is assigned. With these labels, an image is partitioned into a meaningful collection of regions and objects. The Gestalt laws in psychology [66-67] have established some fundamental principles for this inference problem. For example, they imply some well-defined perceptual formulations for image segmentation, such as homogeneous, con tinuity and similarity. In the family of region merging techniques, some methods have used statistical similarity tests [86, 89] to decide the merging of regions, where a predicate is defined for making local decisions. These are good examples of considering the homogeneity characteristics within a region, from which we can see that an essential attribute for region merging is the consistency of data elements in the same region. In other words, if neighboring regions share a common consistency property, they should belong to the same group. However, most of the existing region merging

Algorithms cannot guarantee a globally optimal solution of the merging result. As a consequence, the region merging output is over-merged, under-merged or a hybrid case. In this section, we propose a novel predicate which leads to certain global properties for the segmentation result. The proposed predicate is based on measuring the dissimilarity between pixels along the boundary of two regions. For the convenience of expression, we use the definition of region adjacency graph (RAG) [30] to represent an image. Let G = (V, E) be an undirected graph, where vi∈V is a set of nodes corresponding to image elements (e.g. super-pixels or regions). E is a set of edges connecting the pairs of neighboring nodes. Each edge (vi,vj)∈E has a corresponding weight w((vi,vj)) to measure the dissimilarity of the two nodes connected by that edge. In the context of region merging, a region is represented by a component R ⊆ V. We obtain the dissimilarity between two neighboring regions R1, R2 ⊆ V as the minimum weight edge connecting

them. That is,

$$S(R_1, R_2) = \min_{v_i \in R_1, v_j \in R_2, (v_i, v_j) \in E} w((v_i, v_j)) \quad (12)$$

The graph structure of an example partition is shown in Fig. 1, where the image has 7 regions and its RAG is shown on the right. The advantage of RAG is that it can provide a "spatial view" of the image.

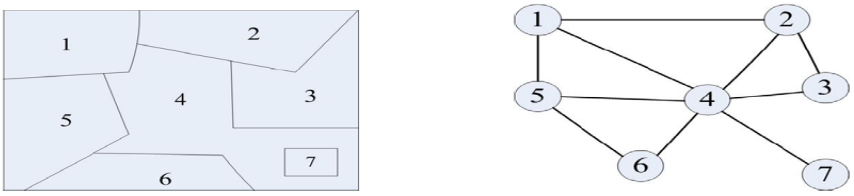

Fig 1. An example of region partition and the corresponding region adjacency graph (RAG).

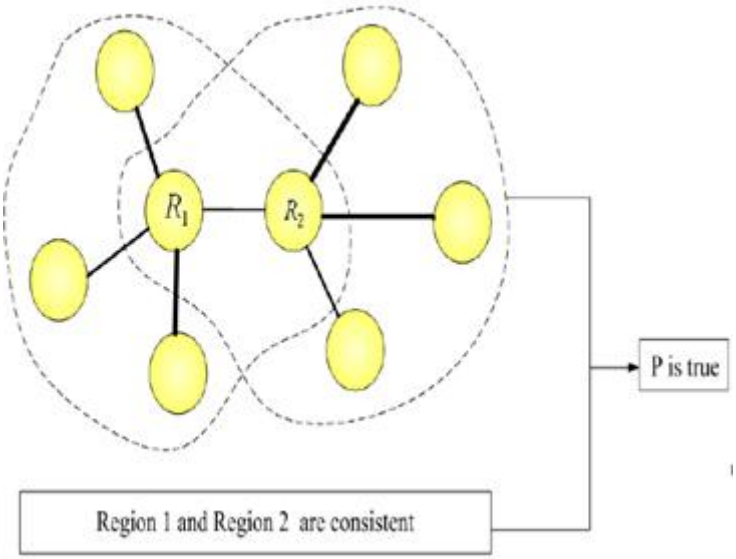

Fig 2. An example that the predicate P between R1 and R2 is true.

The thickness of lines indicates the weights of the edges. The most similar pair of regions is connected by an edge with the minimal weight.

Since the merging predicate will decide whether there is an evidence of merging between the pair of regions, it involves two aspects: a dissimilarity measure which is used to determine the candidate region for merging, and the consistency property which checks if the regions are homogenous. We define the following region merging predicate P:

$$P(R_1, R_2) = \begin{cases} true & \text{if (a) } S(R_1, R_2) = \min_{R_i \in \Omega_1} S(R_1, R_i) = \min_{R_j \in \Omega_2} S(R_2, R_j); \text{ and} \\ & \text{(b) } R_1 \text{ and } R_2 \text{ are consistent} \\ false & \text{otherwise} \end{cases} \quad (13)$$

where Ω1 and Ω 2 are the neighborhood sets of R1 and R2, respectively.[77] The merging predicate on regions R1 and R2 could thus be "merge R1 and R2 if and only if they are the most similar neighbors in each other's neighborhood and follow the principle of consistency." The condition (a) is stronger than that of only requiring the connecting edge between R1 and R2 to be the minimal one in either of the neighborhood. This leads to an interesting property of the proposed region merging algorithm, i.e., the candidates of the pairs of regions for merging are uniquely decided by the given graph. We shall see hereafter that such a condition uniquely decides the pairs of regions to be merged at a given merging level. Moreover, in Section V we will prove that there is always at least one pair of regions which satisfies condition (a). Clearly, without condition (b), all the regions will be merged into one big region at the end of region merging process. Therefore, condition (b) acts as a stopping criterion. Fig. 2 illustrates an example when the predicate P between regions R1 and R2 is true.

1. Consistency Test of Cues

In order to obtain the homogenous regions in region merging, the proposed predicate P in Eq. (13) checks the consistency of regions. Region information is usually presented by the cues extracted from the observed data. The choice of cues can be intensity, color, texture and so on. If we view the cue as a random variable, the distribution of the cue depends on the consistency of pairs of regions. In this paper, we formulate the evaluation of the region consistency as a sequential test process. Suppose parameter θ is related to the distribution of random cues x. More specifically, we gather information of parameter θ by observing random variables in successive steps. Since every sample of the cues carries statistical information on parameter θ, we may collect the information at the end of observation. This is one of the interesting problems studied in sequential analysis, where θ is called a hypothesis. In the context of region merging, two hypotheses are involved in the evaluation task: a pair of regions is "consistent", and is "inconsistent", which are denoted by a null hypothesis H0: θ = θ 0 against an alternative hypothesis H1: θ = θ 1, respectively. The property of the hypotheses is a hidden state that is not directly observable, but is statistically linked to the observable cues. To decide whether or not a pair of regions belongs to the same group, we look for the solution of its hypothesis test. An efficient and popular procedure for integrating the statistical evidence is the sequential probability ratio test (SPRT) which was proposed by Wald [78]. SPRT shows that the solution to the hypothesis can be found by making the smallest number of observations and satisfying the bounds on the predefined probabilities of two errors. SPRT is purely sequential in nature, i.e., continuing sampling on the instances of a random variable will eventually lead to a reliable inference about parameter θ. The application of SPRT to the consistency test of cues is described as follows. We observe the distribution of random cues x in a sequence until a likelihood ratio δ goes out of the interval (B, A) for the first time by a random walk, where the real numbers A and B satisfy B<0<A. The sequence of successive likelihood ratio δ i is:

$$\delta_i = \log \frac{P_0(x_i \mid \theta_0)}{P_1(x_i \mid \theta_1)}, \quad i = 1, 2, \cdots, N \tag{14}$$

where P0(x| θ 0) and P1(x| θ 1) are the distributions of visual cues. P0(x| θ 0) and P1(x| θ 1) should be different so as to make a convincing decision. We use the Gaussian distribution model to approximate the cue distributions. The two conditional probabilities are given as follows:

$$\begin{cases} P_0(x \mid \theta_0) = \lambda_1 \exp(-(I_b - I_{a+b})^T S_I^{-1} (I_b - I_{a+b})) \\ P_1(x \mid \theta_1) = 1 - \lambda_2 \exp(-(I_b - I_a)^T S_I^{-1} (I_b - I_a)) \end{cases} \tag{15}$$

where Ia and Ib are the average color of sampled data in regions a and b respectively, and Ia+b is the average value of samples' union. SI is the covariance matrix of the regions, and λ 1 and λ 2 are scalar parameters. If each test is independent, the composition of the likelihood ratios is the sum of the individual δ i:

$$\delta = \sum_{i=1}^{N} \delta_i \tag{16}$$

where N is the first integer for which δ ≥ A or δ ≤ B. We can see that the solution to the hypothesis is decided by the relationship between δ, an upper limit and a lower limit, denoted by A and B, respectively. If δ goes out of one of these limits, the hypothesis is made and thus the test stops. Otherwise, the test is carried on with a new random sampling.

Algorithm 1: consistency test of cues

Preset λ 1;

Let λ 2 =1, α=0.05, β=0.05;

Compute parameters:

N0: be a constant greater than max{E{δ | θ 0}, E{δ | θ 1}};

A=log(1-β)/α , B=logβ(1-α);

P0(x| θ 0), P1(x| θ 1) are computed using Eq. (4).

Input: a pair of neighboring regions.

Output: the decision D that the two regions are "consistent" (D=1) or "inconsistent" (D=0).

1. Set evidence accumulator δ and the trials counter n to be 0.
2. Randomly choose m pixels in each of the pair of regions, where m equals the half size of the region.
3. Calculate the distributions of visual cues x using Eq. (4) based on these pixels.
4. Update the evidence accumulator

$$\delta = \delta + \log \frac{P_0(x_i \mid \theta_0)}{P_1(x_i \mid \theta_1)}.$$

5. If n≤N0 If $\delta \geq A$, return D=1 (consistent)
If $\delta \leq B$, return D=0 (inconsistent)
If n>N0
If $\delta \geq 0$, return D=1 (consistent)
If $\delta <0$, return D=0 (inconsistent)
6. Go back to step 2.

2. The dynamic region merging algorithm

In this section, we explain the proposed region merging algorithm as a dynamic region merging (DRM) process, which is proposed to minimize an objective function with the merging predicate P defined in Eq. (13). As mentioned in Section I, the proposed DRM algorithm is started from a set of over-segmented regions. This is because a small region can provide more stable statistical information than a single pixel, and using regions for merging can improve a lot the computational efficiency. For simplicity and in order to validate the effectiveness of the proposed DRM algorithm, we use the watershed algorithm [71] (with some modification) to obtain the initially over-segmented regions (please refer to Section VI-A for more information), yet using a more sophisticated initial segmentation algorithm (e.g. mean-shift [62]) may lead better final segmentation results. Given an over-segmented image, there are many regions to be merged for a meaningful segmentation. By taking the region merging as a labeling problem, the goal is to assign each region a label such that regions belong to the same object will have the same label. There are two critical labels for a region Ri: the initial label li 0, which is decided by the initial segmentation, and the final label li n, which is assigned to the region when the merging process stops. In our problem, the final label li n for a given region is not unique, which means that the same initialization li 0 could lead to different solutions. This uncertainty mainly comes from the process of SPRT with a given decision error. The test of consistency/inconsistency depends on the error probabilities of the cue decisions α and β. In general, these decisions are precise for homogenous regions. If a region contains a small part of non-homogenous data, the SPRT might add a few more times of tests to verify its decision. With reasonably small error probabilities, the segmentation results will be more reliable. According to our observation, in most cases, the segmentation result is stable for a given image and it can be guaranteed that all the results satisfy the merging predicate P defined in Eq. (2). In the process of region merging, the label of each region is sequentially transited from the initial one to the final one, which is denoted as a sequence $(l_i^0, l_i^1, \ldots, l_i^n)$. To find an optimal sequence of merges which produce a union of optimal labeling for all regions, the minimization of a certain objective function F is required. According to predicate P, the transition of a region label to another label corresponds to a minimal edge weight that connects the two regions. In this case, a sequence of transitions will be defined on a set of local minimum weights, i.e., in each transition the edge weight between the pair of merged regions should be the minimal one in the neighborhood. As a result, the objective function F used in this work is defined as the measure of transition costs in the space of partitions. In other words, as the whole image is a union of all regions, F is the sum of transition costs over all regions. That is:

$$F = \sum_{R_i} F_i \tag{17}$$

Where Fi is the transition costs of one region Ri in the initial segmentation. Minimizing F in Eq. (17) is a combinatorial optimization problem and finding its global solution is in general a hard task. Since the exhaustive search in the solution space is impossible, an efficient approximation method is desired. The solution adopted here is based on the stepwise minimization of F, where the original problem is broken down into several sub-problems by using the dynamic programming (DP) technique [73]. The DP is widely used to find the (near) optimal solution of many computer vision problems. The principle of DP is to solve a problem by studying a collection of sub-problems. Indeed, there have been some works in image segmentation that benefit from this efficient optimization technique, such as DP snake [64-65]. In the proposed DRM algorithm, we apply DP on discrete regions instead of line segments. The minimization problem for region Ri starting at labeling li 0 is defined as:

$$\begin{aligned} \min F_i(l_i^0, \cdots, l_i^n) &= \min F_i(l_i^0, l_i^{n-1}) + d_{n-1,n} \\ &= \min F_i(l_i^0, l_i^{n-2}) + d_{n-2,n-1} + d_{n-1,n} \\ &= \cdots \\ &= \sum_{k=0}^{n-1} d_{k,k+1} \end{aligned} \tag{18}$$

Where $F_i(l_i^0, l_i^1, \ldots, l_i^n)$ is the transition cost from l_i^0 to l_i^n, dk,k+1 is the minimal edge weight between the regions with labeling l_i^k and l_i^{k+1}, respectively. In conjunction with Eq. (12), we have

$$d_{k,k+1} = \min_{R_{k+1} \in \Omega_k} S(R_k, R_{k+1}) \tag{19}$$

The overall path length from l_i^0 to l_i^n n is the sum of minimum edges dk,k+1 for each node in that path. This problem reduces to a search for a shortest path problem, whose solution can be found at a finite set of steps by the Dijkstra's algorithm in polynomial time. At this point, a minimization process of objective function F is exactly described by the predicate P defined in Eq. (13), where P is true if the nodes are connected by the edge with the minimal weight in their neighborhood. It means that the closest neighbors will be assigned to the same label, which is the cause of the merging. In Fig. 3, an example process of region merging is shown by embedding it into a 3D graph. Between two adjacent layers there is a transition which indicates the costs of a path. Clearly, this is also a process of label transitions.[92] The neighborhood of the highlighted region (in red) is denoted as the black nodes in the graph and the closest neighbor is denoted as the red nodes. The directed connections with the lowest cost between adjacent layers are made (shown as blue arrows). Note that the connectivity between regions in the same layer is represented by the RAG, which is not explicitly shown in Fig.3.

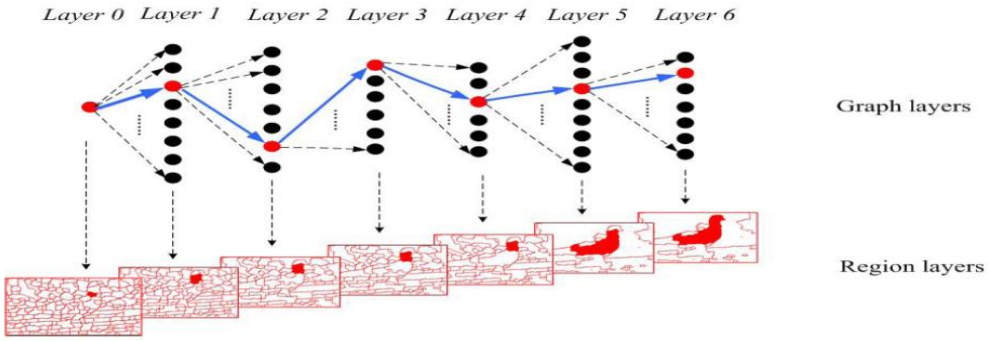

Fig 3. The dynamic region merging process as a shortest path in a layered graph.

The upper row shows the label transitions of a graph node. The lower row shows the corresponding image regions of each label layer. Starting from layer 0, the highlighted region (in red) obtains a new label from its closest neighbor (in red). If the region is merged with its neighbor, they will be assigned to the same label. The shortest path is shown as the group of the directed edges (in blue).

Algorithm 2: segmentation by dynamic region merging

Input: the initially over segmented image S0.

Output: region merging result.

1. Set i=0.
2. For each region in segmentation Si, use **Algorithm 1** to check the value of predicate P with respect to its neighboring regions.
3. Merge the pairs of neighboring regions whose predicate P is true, such that segmentation Si+1 is constructed.
4. Go back to step 2 until Si+1 = Si.
5. Return Si.

V. CONCLUSIONS

In this paper, we have proposed a Bayesian approach to perform simultaneously image registration and pixel classification. The proposed technique is well-suited to deal with image pairs that contain two classes of pixels with different inter-image intensity relationships. We have shown through different experiments that the model can be applied in many different ways. For instance if the class map is known, then it can be used for template-based segmentation. If the full model is used (estimation of the class map, the registration and the parameters of the distribution of the outliers), then it can be applied to lesion detection by image comparison. In

this paper, we proposed a novel method for segmenting an image into distinct components. The proposed algorithm is implemented in a region merging style. We defined a merging predicate P for the evidence of a merging between two neighboring regions. This predicate was defined by the sequential probability ratio test (SPRT) and the maximum likelihood criterion. A dynamic region merging (DRM) was then presented to automatically group the initially over-segmented many small regions. Although the merged regions are chosen locally in each merge stage, some global properties are kept in the final segmentations. For the computational efficiency, we introduced an accelerated algorithm by using the data structure of region adjacency graph (RAG) and nearest neighbor graph (NNG). Experiments on natural images showed the efficiency of the proposed algorithm. There are several potential extensions to this work, such as the introduction of global refinement and user interaction, etc. Those will be further investigated in our future work.

REFERENCES

[1]. L. Brown, "A survey of image registration techniques," ACM Computing Surveys, vol. 24, pp. 325–376, 1992.

[2]. D. Hill, P. Batchelor, M. Holden, and D. J. Hawkes, "Medical image registration," Physics in Medicine and Biology, vol. 46, no. 3, pp. R1–R45, 2001.

[3]. J. Maintz and M. Viergever, "A survey of medical image registration," Medical Image Analysis, vol. 2(1), pp. 1–36, 1998.

[4]. P. Pluim, J. Maintz, and M. Viergever, "Mutual-information based registration of medical images : a survey," IEEE Transactions on Medical Imaging, vol. 22, no. 8, pp. 986–1004, 2003.

[5]. J. Modersitzki, Numerical Methods for Image Registration, ser. Numerical Mathematics And Scientific Computation, C. S. G. H. Golub and E. Suli, Eds. Oxford University Press, 2004.

[6]. R. Woods, J. Mazziotta, and S. R. Cherry, "MRI-PET registration with automate algorithm," Journal of Computer Assisted Tomography, vol. 17, no. 4, pp. 536–46, Jul-Aug 1993.

[7]. T. M. Buzug and J. Weese, "Voxel-based similarity measures for medical image registration in radiological diagnosis and image guided surgery," Journal of Computing and Information Technology, vol. 6, no. 2, pp. 165–179, 1998.

[8]. A. Roche, G. Malandain, X. Pennec, and N. Ayache, "The correlation ratio as a new similarity measure for multimodal image registration," in First Int. Conf. on Medical Image Computing and Computer-Assisted Intervention (MICCAI'98). vol. LNCS 1496. Cambridge, USA: Springer Verlag, October 1998, pp. 1115–1124.

[9]. C. Studholme, D. Hill, and D. J. Hawkes, "An overlap invariant entropy measure of 3D medical image alignment," Pattern Recognition, vol. 1, no. 32, pp. 71–86, 1999.

[10]. A. Roche, G. Malandain, and N. Ayache, "Unifying Maximum Likelihood Approaches in Medical Image Registration," International Journal of Computer Vision of Imaging Systems and Technology, vol. 11, pp. 71–80, 2000.

[11]. G. Malandain, "Les mesures de similarit´e pour le recalage des images m´edicales," Habilitation `a Diriger des Recherches, Universit´e de Nice Sophia-Antipolis, 2006.

[12]. P. Hayton, M. Brady, L. Tarassenko, and N. Moore, "Analysis of dynamic MR breast images using a model of contrast enhancement," Medical Image Analysis, vol. 1, pp. 207–224, 1997.

[13]. C. Tanner, J. A. Schnabel, D. Chung, M. J. Clarkson, D. Rueckert, D. Hill, and D. J. Hawkes, "Volume and shape preservation of enhancing lesions when applying non-rigid registration to a time series of contrast enhancing MR breast images," in MICCAI '00: Proceedings of the Third International Conference on Medical Image Computing and Computer- Assisted Intervention, London, UK, 2000, pp. 327–337.

[14]. T. Rohlfing and C. R. Maurer, Jr., "Intensity-based non-rigid registration using adaptive multilevel free-form deformation with an incompressibility constraint," in Proceedings of Fourth International Conference on Medical Image Computing and Computer-Assisted Intervention (MICCAI 2001), ser. Lecture Notes in Computer Science, W. Niessen and M. A. Viergever, Eds., vol. 2208. Berlin: Springer-Verlag, 2001, pp. 111–119. N. Sebe and M. Lew, Robust Computer Vision: Theory and Applications. Series: Computational Imaging and Vision, 2003, vol. 26.

[15]. P. Rousseeuw and A. Leroy, Robust Regression and Outlier Detection. Wiley, New York, 1987.

[16]. F. Hampel, E. Ronchetti, P. Rousseeuw, and W. Stahel, Robust Statistics: The Approach Based on Influence Functions. Wiley, New York, 1986.

[17]. D. Hawkins, Identifications of Outliers. Chapman & Hall, London, New York, 1980.

[18]. P. Huber, Robust Statistics. Wiley, New York, 1981.

[19]. F. Richard, "A new approach for the registration of images with inconsistent differences," in Proc. of the Int. Conf. on Pattern Recognition, ICPR, vol. 4, Cambridge, UK, 2004, pp. 649–652.

[20]. C. Nikou, F. Heitz, and J.-P. Armspach, "Robust voxel similarity metrics for the registration of dissimilar single and multimodal images," Pattern Recognition, vol. 32, pp. 1351–1368, 1999.
[21]. J. Kim, "Intensity based image registration using robust similarity measure and constrained optimization: Applications for radiation therapy," Ph.D. dissertation, University of Michigan, 2004.
[22]. M. Black, "Robust incremental optical flow," Ph.D. dissertation, Yale University, New Haven, CT, USA, 1992.
[23]. P. Meer, D. Mintz, A. Rosenfeld, and D. Kim, "Robust regression methods for computer vision: A review," International Journal of Computer Vision, vol. 6, no. 1, pp. 59–70, 1991.
[24]. M. Black and A. Rangarajan, "On the unification of line processes, outlier rejection, and robust statistics with applications in early vision," International Journal of Computer Vision, vol. 19, no. 1, pp. 57–91, 1996.
[25]. N. S. Netanyahu and I. Weiss, "Analytic outlier removal in line fitting," in 12th IAPR International Conference on Computer Vision and Image Processing, vol. 2B, 1994, pp. 406–408.
[26]. P. Schroeter, J.-M. Vesin, T. Langenberger, and R. Meuli, "Robust parameter estimation of intensity distributions for brain magnetic resonance images," IEEE Transactions on Medical Imaging, vol. 17, no. 2, pp. 172–186, 1998.
[27]. P. S. Torr, R. Szeliski, and P. Anandan, "An Integrated Bayesian Approach to Layer Extraction from Image Sequences," IEEE Transactions on Pattern Analysis and Machine Intelligence, vol. 23, no. 3, pp. 297–303, 2001.
[28]. D. Hasler, L. Sbaiz, S. Susstrunk, and M. Vetterli, "Outlier modeling in image matching," IEEE Transactions on Pattern Analysis and Machine Intelligence, pp. 301–315, 2003.
[29]. P. Biber, S. Fleck, and W. Straßer, "A probabilistic framework for robust and accurate matching of point clouds," in 26th Pattern Recognition Symposium (DAGM 04), 2004.
[30]. A. Jepson and M. Black, "Mixture models for optical flow computation," in IEEE Conference on Computer Vision andPattern Recognition, 1993, pp. 760–761.
[31]. M. Hachama, A. Desolneux, and F. Richard, "Combining registration and abnormality detection in mammography," in Workshop on Biomedical Image Registration, (WBIR'2006), ser. Lecture Notes in Computer Science, J. Pluim, B. Likar, and F. Gerritsen, Eds., vol. 4057. Springer, 2006, pp. 178–185.
[32]. H. Hachama, F. Richard, and A. Desolneux, "A mammogram registration technique dealing with outliers," in Proc. of the IEEE International Symposium on Biomedial Imaging (ISBI'2006), 2006, pp. 458–461.
[33]. M. Hachama, F. Richard, and A. Desolneux, "A probabilistic approach for the simultaneous mammogram registration and abnormality detection," in International Workshop on Digital Mammography (IWDM'2006), ser. Lecture Notes in Computer Science, S. Astley, M. Brady, C. Rose, and R. Zwiggelaar, Eds., vol. 4046. Springer, 2006, pp. 205–212.
[34]. N. Rougon, A. Discher, and F. Preteux, "Region-driven statistical non-rigid registration: application to model-based segmentation and tracking of the heart in perfusion MRI," in Proceedings SPIE Conference on Mathematical Methods in Pattern and Image Analysis, vol. 5916, San Diego, August 2005, pp. 148–159.
[35]. C. Studholme, D. Hill, and D. J. Hawkes, Eds., Incorporating Connected Region Labeling into Automated Image Registration Using Mutual Information, ser. Proceedings of the IEEE workshop on Mathematical Methods in Biomedical Image Analysis, San Francisco Ca. IEEE Computer Society Press, 1996.
[36]. J. Chappelow, B. Bloch, N. Rofsky, E. Genega, R. Lenkinski, W. DeWolf, and A. Madabhushi, "Elastic registration of multimodal prostate mri and histology via multiattribute combined mutual information." Med Phys, vol. 38, no. 4, pp. 2005–18, 2011.
[37]. P. Patel, J. Chappelow, J. Tomaszewski, M. Feldman, M. Rosen, N. Shih, and A. Madabhushi, "Spatially weighted mutual information (SWMI) for registration of digitally reconstructed ex vivo whole mount histology and in vivo prostate MRI," in IEEE International Conference of Engineering in Medicine and Biology Society (EMBS), 30 2011-sept. 3 2011, pp. 6269 –6272.
[38]. M. Hachama, A. Desolneux, C. Cuenod, and F. Richard, "A classifying registration technique for the estimation of enhancement curves of DCE-CT scan sequences," Medical Image Analysis, vol. 14, no. 2, pp. 185 – 194, 2010.
[39]. J. Ashburner and K. Friston, "Unified segmentation," NeuroImaging, vol. 26, pp. 839–851, 2005.
[40]. K. Pohl, J. Fisher, W. Grimson, R. Kikinis, and W. Wells, "A Bayesian model for joint segmentation and registration," NeuroImage, vol. 31, no. 1, pp. 228–239, 2006.
[41]. P. Wyatt and A. Noble, "MAP MRF Joint Segmentation and Registration of Medical Images," Medical Image Analysis, vol. 7, no. 4, pp. 539–552, 2003.

[42]. C. Xiaohua, M. Brady, J. L.-C. Lo, and N. Moore, "Simultaneous segmentation and registration of contrast-enhanced breast MRI," in Information Processing in Medical Imaging, 2005, pp. 126–137.
[43]. Y. Zheng, J. Yu, C. Kambhamettu, S. Englander, M. Schnall, and D. Shen, "De-enhancing the Dynamic Contrast-Enhanced Breast MRI for Robust Registration," in MICCAI, ser. Lecture Notes in Computer Science, N. Ayache, S. Ourselin, and A. Maeder, Eds., vol. 4791. Springer, 2007, pp. 933–941.
[44]. D. Mumford, "The Bayesian rationale for energy functionals," Geometry-driven Diffusion in Computer Vision, vol. 46, pp. 141–153, 1994.
[45]. C. A. Glasbey and K. V. Mardia, "A review of image-warping methods," Journal of Applied Statistics, vol. 25, no. 2, pp. 155–171, April 1998.
[46]. C. Broit, "Optimal registration of deformed images," Ph.D. dissertation, University of Pennsylvania, Philadelphia, 1981.
[47]. R. Bajcsy, R. Lieberson, and M. Reivich, "Computerized system for the elastic matching of deformed radiographic images to idealized atlas images," Journal of Computer Assisted Tomography, vol. 7, 1983.
[48]. R. Bajcsy and S. Kovacic, "Multiresolution elastic matching," Computer Vision, Graphics, and Image Processing, vol. 46, no. 1, pp. 1–21, 1989.
[49]. M. Miller, G. Christensen, Y. Amit, and U. Grenander, "Mathematical textbook of deformable neuroanatomies," Proc. Of the National Academy of Sciences, vol. 90, pp. 11 944–11 948, 1993.
[50]. Y. Amit, U. Grenander, and M. Piccioni, "Structural image restoration through deformable templates," American Statistical Association, vol. 86, no. 414, June 1991.
[51]. F. L. Bookstein, "Principal warps: Thin-plate splines and the decomposition of deformations," IEEE Transactions on Pattern Analysis and Machine Intelligence, vol. 11, no. 6, pp. 567–585, 1989.
[52]. S. Allassonni`ere, Y. Amit, and A. Trouv´e, "Towards a coherent statistical framework for dense deformable template estimation," Journal Of The Royal Statistical Society Series B, vol. 69, no. 1, pp. 3–29, 2007.
[53]. F. Richard, A. Samson, and C. Cuenod, "A SAEM algorithm for the estimation of template and deformation parameters in medical image sequences," Statistics and Computing, vol. 19, no. 4, pp. 465–478, 2009.
[54]. S. Geman and D. Geman, "Stochastic relaxation, Gibbs distributions, and the Bayesian restoration of images," IEEE Transactions on Pattern Analysis and Machine Intelligence, vol. 6, pp. 721–741, 1984.
[55]. B. Chalmond, Modelling and inverse problems in image analysis, ser. Applied mathematical sciences, Kindle, Ed. Springer, 2003, vol. 155.
[56]. M. Staring, S. Klein, and J. Pluim, "Nonrigid registration with tissue-dependent filtering of the deformation field," Physics in Medicine and Biology, vol. 52, pp. 6879–6892, 2007.
[57]. P. G. Ciarlet, The Finite Element Method for Elliptic Problems. Amsterdam: North-Holland Publishing Co., 1978.
[58]. J. Bonnans, J. Gilbert, C. Lemar´echal, and C. Sagastiz´abal, Numerical Optimization – Theoretical and Practical Aspects, ser. Universitext. Springer Verlag, Berlin, 2006.
[59]. D.A. Forsyth and J. Ponce, Computer Vision: A Modern Approach. Prentice Hall, 2002
[60]. L. Ladicky, C. Russell, P. Kohli, P. Torr. Associative Hierarchical CRFs for Object Class Image Segmentation. In: ICCV 2009.
[61]. F, Lecumberry, A, Pardo and G. Sapiro. Simultaneous object classification and segmentation with high-order multiple shape models. IEEE Transactions on Image Processing. pp: 625 - 635, 2010.
[62]. R.C. Gonzalez and R.E. Woods. Digital Image Processing. Addison Wesley, Reading, MA, 1992.
[63]. J. Canny. A Computational Approach to Edge Detection, IEEE Trans. Pattern Analysis and Machine Intelligence, vol. 8, pp. 679-698, 1986.
[64]. B. Paul, L. Zhang and X. Wu, "Canny edge detection enhancement by scale multiplication," IEEE. Trans. on Pattern Analysis and Machine Intelligence, vol. 27, pp. 1485-1490, Sept. 2005.
[65]. L. Zhang, B. Paul, et al, "Edge detection by scale multiplication in wavelet domain," Pattern Recognition Letters, vol. 23, pp. 1771-1784, 2002.
[66]. J. Shi and J. Malik. Normalized Cuts and Image Segmentation. IEEE Transactions on Pattern Analysis and Machine Intelligence (PAMI) 2000.
[67]. S. Wang, J. M. Siskind. Image Segmentation with Ratio Cut, IEEE Transactions on Pattern Analysis and Machine Intelligence, 25(6):675-690, 2003.
[68]. Z. Wu and R. Leahy. An optimal graph theoretic approach to data clustering Theory and its application to image segmentation. IEEE Transactions on Pattern Analysis and Machine Intelligence. November 1993.

[69]. H. D Cheng, Y. Sun. A hierarchical approach to color image segmentation using homogeneity. IEEE Transactions on Image Processing. Volume: 9 , Issue: 12, page(s): 2071-2082, 2000.
[70]. S. Lee; M.M. Crawford. Unsupervised multistage image classification using hierarchical clustering with a bayesian similarity measure. IEEE Transactions on Image Processing. Page(s): 312 -320, 2005.
[71]. A. Moore, S. J. D. Prince, J. Warrell, U. Mohammed, and G. Jones. Superpixel lattices. CVPR, 2008.
[72]. A. Moore, S. J. D. Prince, J. Warrell, U. Mohammed, and G. Jones. Scene shape priors for superpxiel segmentation. ICCV, 2009.
[73]. A. Moore, S. Prince . "Lattice Cut" - Constructing superpixels using layer constraints. CVPR 2010.
[74]. R. Nock and F. Nielsen. Statistic region merging. IEEE Trans. on Pattern Analysis and Machine Intelligence, vol 26, pages 1452-1458, 2004.
[75]. K. Haris and S. N. Estradiadis and N. Maglaveras and A. K. Katsaggelos. Hybrid image segmentation using watersheds and fast region merging. IEEE Transactions on Image Processing, vol 7, pp. 1684-1699, Dec. 1998.
[76]. P.F. Felzenszwalb and D.P. Huttenlocher. Efficient Graph-Based Image SegmentationInternational Journal of Computer Vision. Vol. 59, Number 2, September 2004.
[77]. B. Peng, L. Zhang and J. Yang, Iterated Graph Cuts for Image Segmentation. In Asian Conference on Computer Vision, 2009.
[78]. Moscheni, F. Bhattacharjee, S. Kunt, M. Spatio-temporal segmentation based on region merging. IEEE Transactions on Pattern Analysis and Machine Intelligence. Vol. 20, pages: 897-915. Sep 1998.
[79]. J. Ning, L. Zhang, D. Zhang and C. Wu. Interactive Image Segmentation by Maximal Similarity based Region Merging. Pattern Recognition, vol. 43, pp. 445-456, Feb, 2010.
[80]. F. Calderero, F. Marques. Region merging techniques using information theory statistical measures. IEEE Transactions on Image Processing. Volume: 19 , Issue: 6. page(s): 1567-1586, 2010.
[81]. F. Calderero, F. Marques. General region merging approaches based on information theory statistical measures. The 15th IEEE International Conference on Image Processing (ICIP). pp: 3016-3019, 2008.
[82]. H. Liu, Q. Guo, M, Xu, I. Shen. Fast image segmentation using region merging with a k-Nearest Neighbor graph. IEEE Conference on Cybernetics and Intelligent Systems. Page(s): 179-184, 2008.
[83]. Y. Shu, G. A. Bilodeau, F. Cheriet. Segmentation of laparoscopic images: integrating graph-based segmentation and multistage region merging. The 2nd Canadian Conference on Computer and Robot Vision, 2005.
[84]. I.E. Gordon, Theories of Visual Perception, first ed. John Wiley and Sons, 1989.
[85]. K. Koffka. Principles of Gestalt Psychology. New York: Harcourt, Brace and World. 1935.
[86]. A. Wald. Sequential Analysis. Wiley Publications in Statistics, Third ed. Wiley, 1947.
[87]. Z. Wu, Homogeneity testing for unlabeled data: A performance evaluation, CVGIP: Graph. Models Image Process., vol. 55, pp. 370-380, Sept. 1993.
[88]. A. Trémeau and P. Colantoni. Regions adjacency graph applied to color image segmentation. IEEE Transactions on Image Processing. Vol. 9, pp. 735-744, 2000.
[89]. L. Vincent, P. Soille, Watersheds in digital spaces: an efficient algorithm based on immersion simulations, IEEE Transactions on Pattern Analysis and Machine Intelligence 13 (6) 583–598, 1991.
[90]. D. Comanicu, P. Meer. Mean shift: A robust approach toward feature space analysis. IEEE Trans. On Pattern Analysis and Machine Intelligence, 24, 603-619, May 2002.
[91]. Bellman, Richard, Dynamic Programming, Princeton University Press, 1957.